Electronic Supplementary Material (ESI) for Inorganic Chemistry Frontiers.

Electronic Supporting Information

Thiol Decorated Defective Metal-Organic Framework Embedded with Palladium Nanoparticles for Efficient Cr(VI) Reduction.

Asha Pankajakshan,[a] Aparna Ravarikkandy,[a] Balu P. Ratheesh,[a] Manju P. Maman,[a] Sukhendu Mandal*[a]

[a]School of Chemistry, Indian Institute of Science Education and Research Thiruvananthapuram, Kerala, India-695551. Email: sukhendu@iisertvm.ac.in

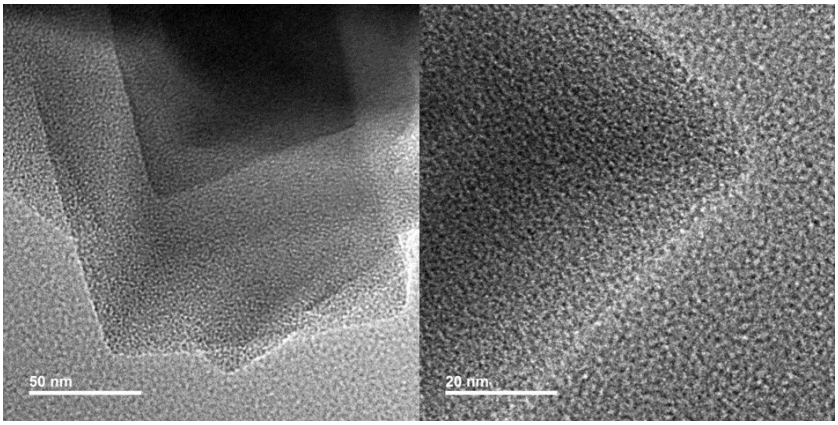

(a)

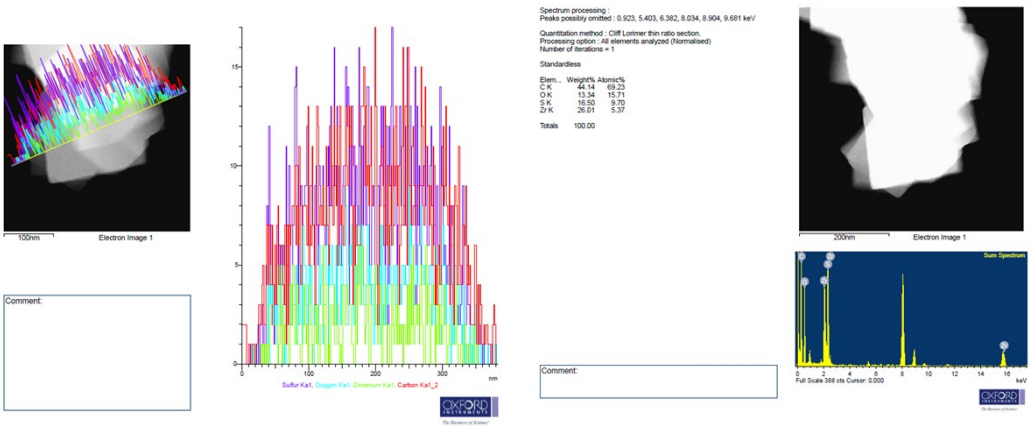

(b) **(c)**

Figure S1. (a) TEM inages of of the –SH incorporated UiO-66, (b) and (c) TEM- EDX spectra of the samples. Note: Presence of sulfur atom supports the incorporation of –SH group in the structure.

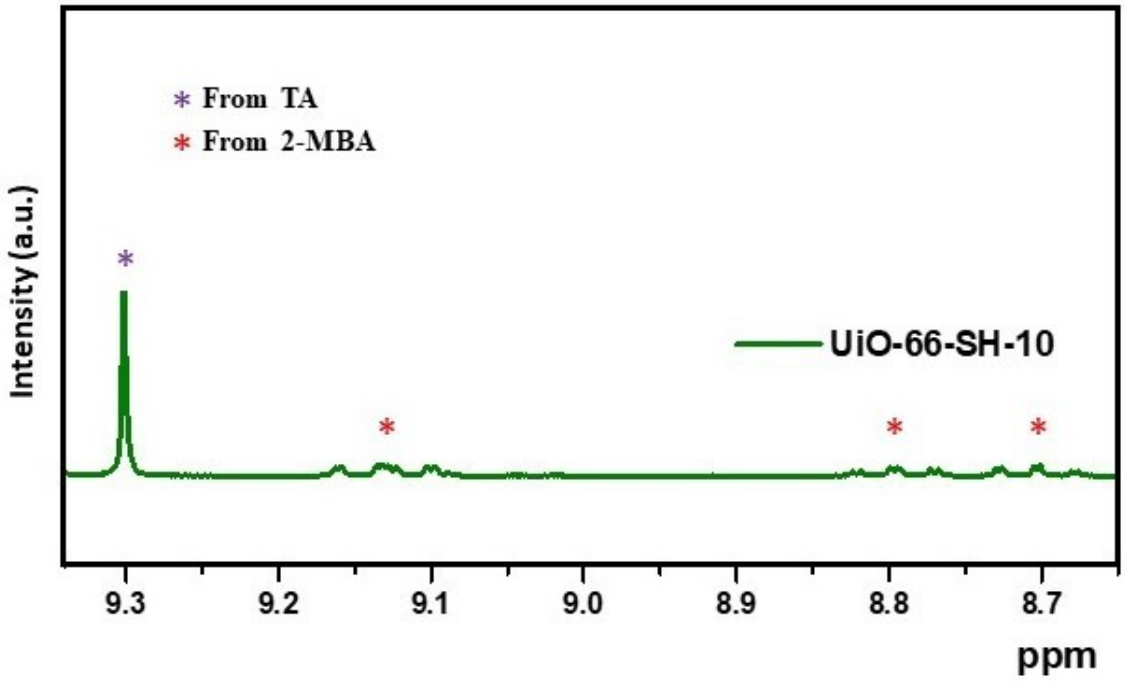

Figure S2. The ^{1}H NMR spectra of UiO-66-SH .

Table S1. The molar ratio of 2-MBA in UiO-66-SH.

MOF	2-MBA/TA
UiO-66-SH-10	0.41

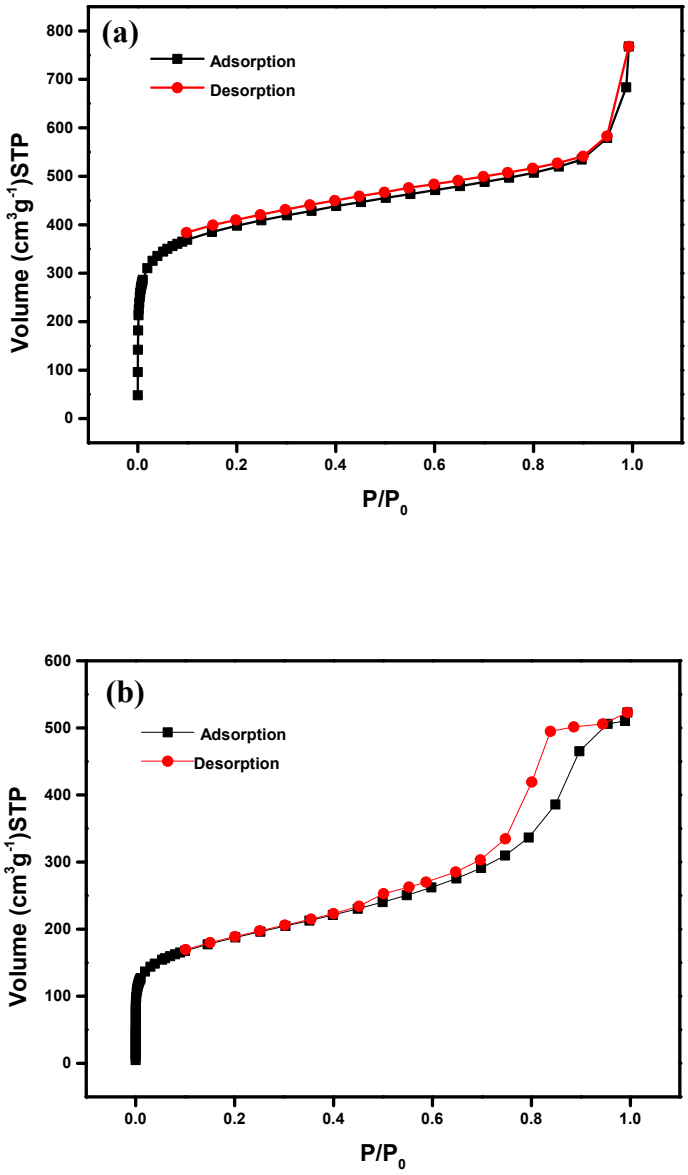

Figure S3. N_2 adsorption-desorption spectra of (a) UiO-66-SH-10 and (b) Pd@ UiO-66-SH-10.

Elem...	Weight%	Atomic%
C K	16.59	42.07
O K	13.92	26.50
S K	14.12	13.42
Zr K	45.31	15.13
Pd L	10.06	2.88
Totals	100.00	

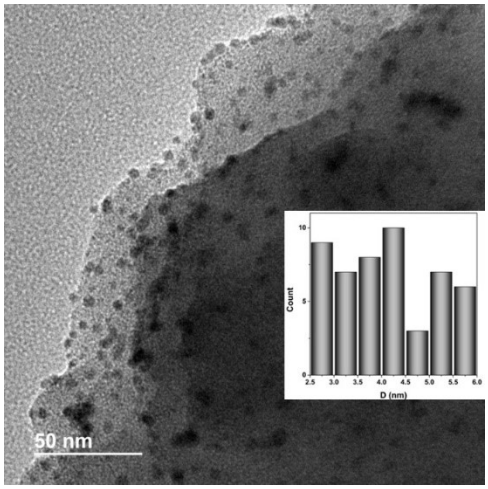

(a) (b)

Figure S4. (a) Percentage of elements present in the Pd@UiO-66-SH; (b) TEM images of as-synthesized Pd@UiO-66-SH. Inset: Histrogram showing particles size.

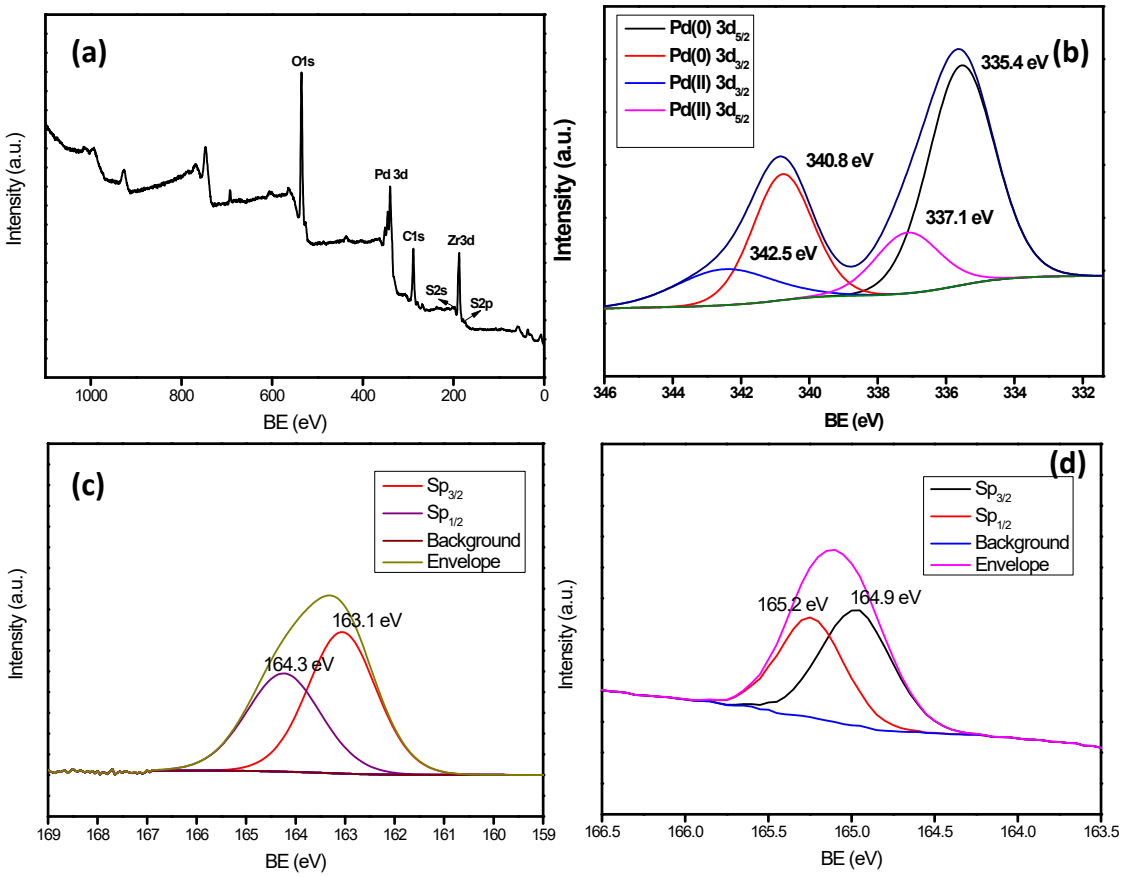

Figure S5. (a) XPS survey spectra, the binding energy of (b) Pd and (c & d) S. Note: Deconvulation showed that 77.5 % Pd in is in metallic state and 22.5 % is in Pd^{2+} state.

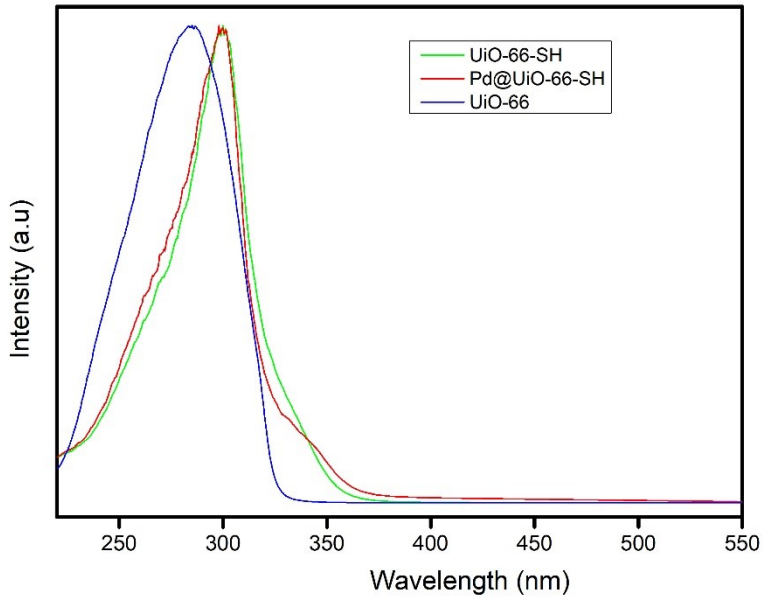

(a)

(b)

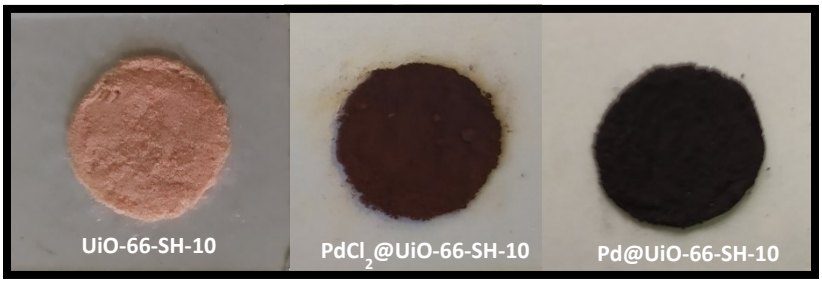

Figure S6. UV-Vis absoprtion spectra of different samples in solid state; (b) color of the respective samples under visible light.

(a) **(b)** **(c)**

Figure S7. Colour change of $K_2Cr_2O_7$ (a) before the reaction, (b) after the reaction and (c) after adding excess dilute NaOH solution.

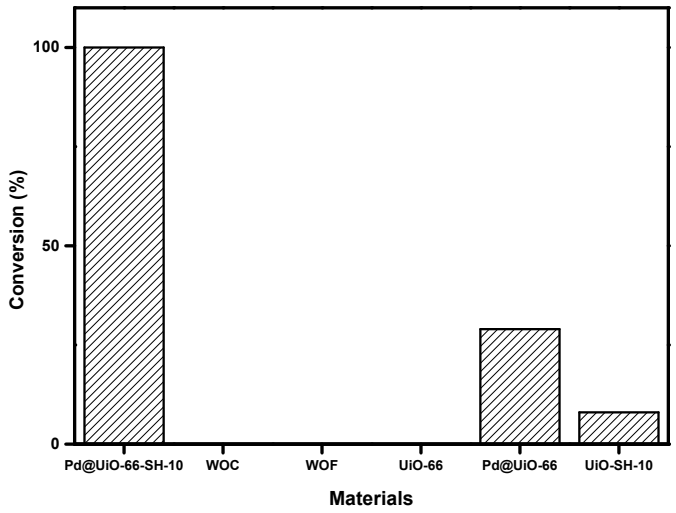

Figure S8. Catalytic conversion of Cr(VI) to Cr(III) with various materials. WOC and WOF are without catalyst and without formic acid, respectively.

Table S2. List of comparative compounds with time taken for the reduction of Cr(VI) to Cr(III) ions.

No	*Catalyst*	*Time(min)*	*References*
1	***Pd@UiO-66-SH-10***	***3***	***This work***
2	*MOF-Titanate nanotube composite*	*20*	*1*
3	*Nanostructured bismuth vanadate*	*160*	*2*
4	*Zr(IV) MOF, JLU-MOF 60*	*70*	*3*
5	*AuPd@Pd NCs*	*3*	*4*
6	*Zn MOF, NNU-36*	*60*	*5*
7	*CuPd alloy nanoparticle*	*7*	*6*
8	*Co-RGO*	*9*	*7*
9	*Pd/GO*	*12-22*	*8*
10	*Pd/Fe-NMC*	*20*	*9*
11	*Mixed metal-MIL-101*	*15-18*	*10*
12	*$Pd@SiO_2–NH_2$*	*6*	*11*
13	*highly reduced {$MnII(P^V_4Mo^V_6O_{31})_2$} clusters*	*240*	*12*
14	*Bi_2S_3/Bi_2WO_6*	*60*	*13*
15	*Ni NP@RGO*	*4*	*14*
16	*RGO/GO-UiO-66-NH2*	*120*	*15*
17	*Pd/Pt/Rh/Au@MIL-101*	*40-210*	*16*
18	*$Pd@UiO-66-NH_2$*	*90*	*17*
19	*Pd@uniform electrospun PEI/PVA nanofibers*	*12*	*18*
20	*$NH_2–MIL-88B$ (Fe)*	*45*	*19*

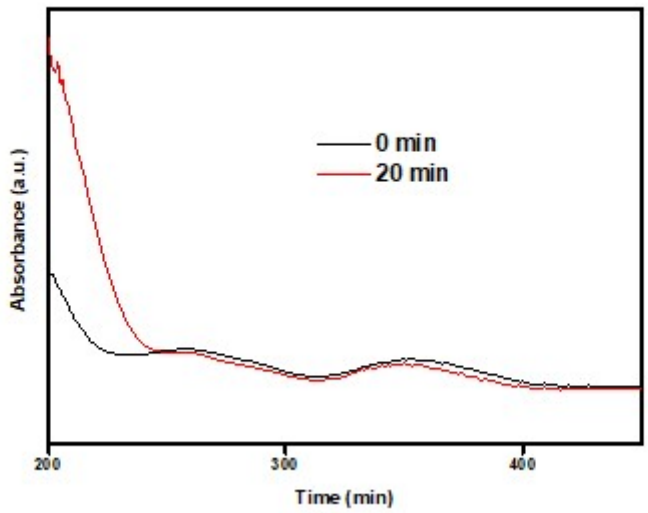

Figure S9. UV-Vis spectra after the leaching test. A fresh amount of Cr(VI) solution was added to the solution after catalysis and monitored the change at 0 and 20 minutes intervals.

Table S3. Concentration of the elements of interest obtained by ICP-MS.

Condition	***Concentration of Pd***	***Concentration of Zr***
Solution obtained after the catalysis	*0 ppm*	*0 ppm*

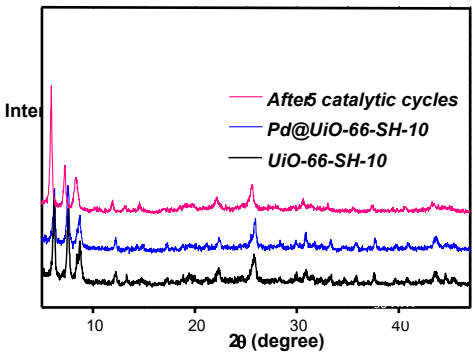

Figure S10. The PXRD pattern before and after 5 cylces of catalysis.

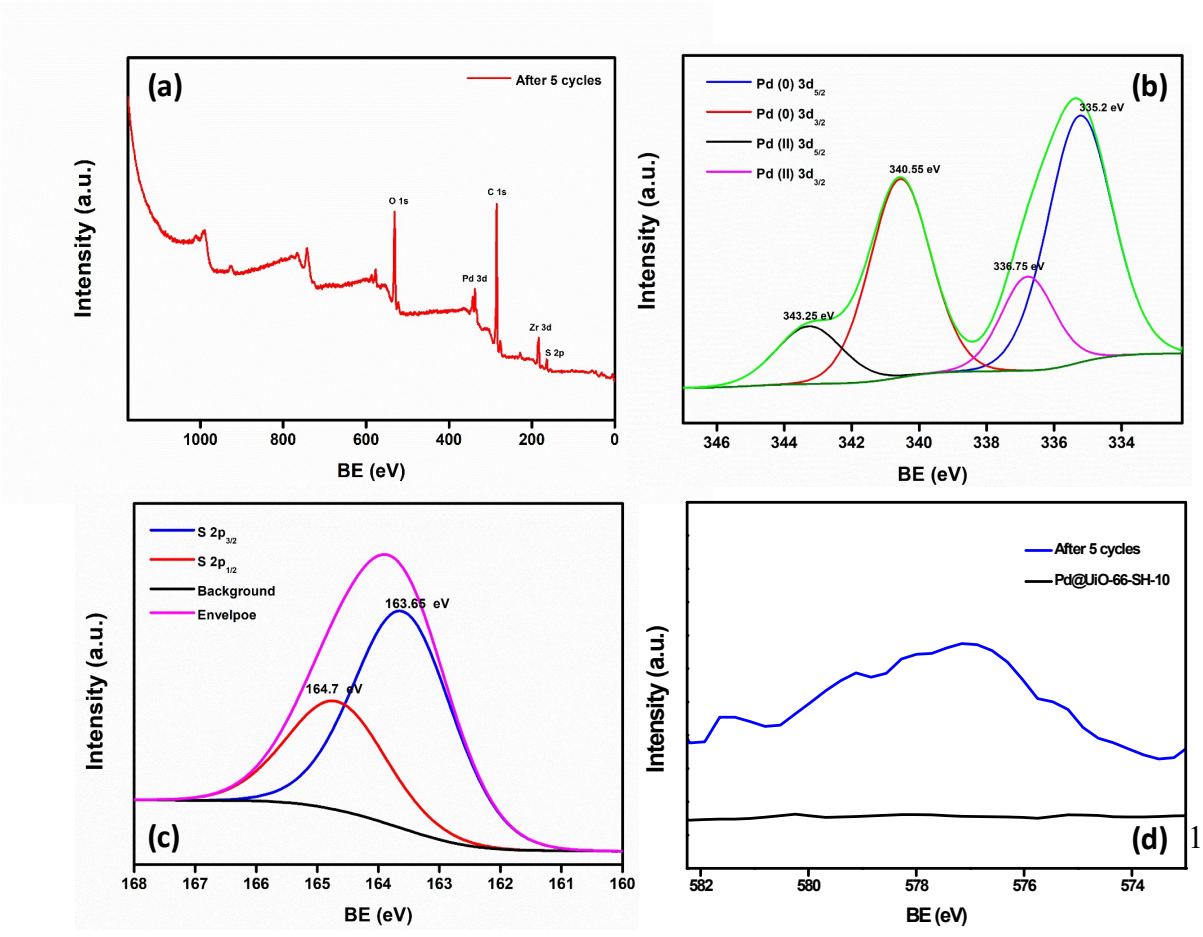

Figure S11. (a) XPS survey spectra, the binding energy of (b) Pd and (c) S, (d) narrow-scan specta of Cr 2p showing the weak peak of the catalyst after 5 catalytic cycles.
Note: Deconvulation showed that 74 % Pd in is in metallic state and 26 % is in Pd^{2+} state.

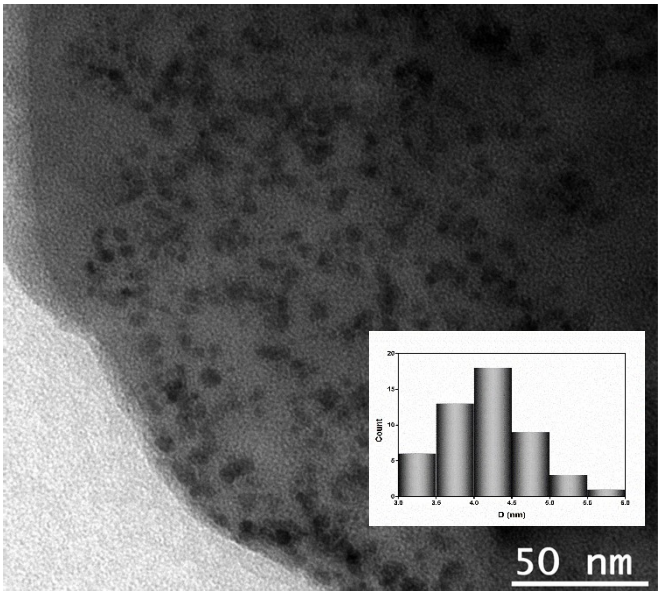

Figure S12. TEM image of Pd@UiO-66-SH after 5 cycles of catalysis. Inset: Histrogram of particles size.

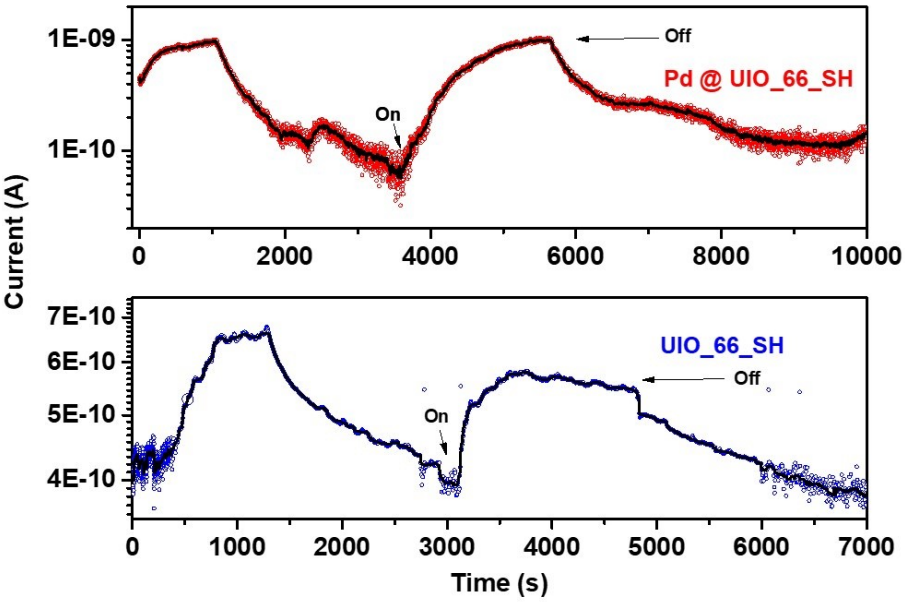

Figure S13. Time-resolved rise and decay curve photocurrent of Pd@UiO-66-SH and UiO-66-SH, respectively.

References:

[1] X. Wang *et al.*, *Environ. Pollut.*, vol. 249, pp. 502–511, 2019.

[2] D. P. Jaihindh, B. Thirumalraj, S. M. Chen, P. Balasubramanian, and Y. P. Fu, *J. Hazard. Mater.*, 2018, **367**, 647–657.

[3] J. Liu *et al.*, *J. Mater. Chem. A*, 2019, **7**, 16833–16841.

[4] F.-Q. Shao, J.-J. Feng, X.-X. Lin, L.-Y. Jiang, and A.-J. Wang, *Appl. Catal. B Environ.*, 2017, 208,128–134.

[5] H. Zhao, Q. Xia, H. Xing, D. Chen, and H. Wang, *ACS Sustain. Chem. Eng.*, 2017, **5**, 4449–4456.

[6] H. Saikia, B. J. Borah, Y. Yamada, and P. Bharali, *J. Colloid Interface Sci.*, 2017, 486, 46–57.

[7] T. Xu, J. Xue, X. Zhang, G. He, and H. Chen, *Appl. Surf. Sci.*, 2017, **402**, 294–300.

[8] M. Celebi, K. Karakas, I. E. Ertas, M. Kaya, and M. Zahmakiran, *ChemistrySelect*, 2017, **2**, 8312–8319.

[9] S. Li *et al.*, *Environ. Sci. Pollut. Res.*, 2016, **23**, 22027–22036.

[10] M. Trivedi, Bhaskaran, A. Kumar, G. Singh, A. Kumar, and N. P. Rath, *New J. Chem.*, 2016, **40**, 3109–3118.

[11] M. Celebi, M. Yurderi, A. Bulut, M. Kaya, and M. Zahmakiran, *Appl. Catal. B Environ.*, 2016, **180**, 53–64.

[12] K. Gong *et al.*, *Eur. J. Inorg. Chem.*, 2015, **32**, 5351–5356.

[13] A. Rauf *et al.*, *ACS Sustain. Chem. Eng.*, 2015, **3**, 2847–2855.

[14] K. Bhowmik, A. Mukherjee, M. K. Mishra, and G. De, *Langmuir*, 2014, **30**, 3209–3216.

[15] L. Shen, L. Huang, S. Liang, R. Liang, N. Qin, and L. Wu, *RSC Adv.*, 2014, **4**, 2546–2549.

[16] M. Yadav and Q. Xu, *Chem. Commun.*, 2013, **49**, 3327–3329.

[17] L. Shen, W. Wu, R. Liang, R. Lin, and L. Wu, *Nanoscale*, 2013, **5**, 9374–9382.

[18] Y. Huang *et al.*, *ACS Appl. Mater. Interfaces*, 2012, **4**, 3054–3061.

[19] L. Shi *et al.*, *Adv. Sci.*, 2015, **2**, 1500006.